Title

Fully coupled wellbore-reservoir simulation of supercritical CO2 injection from fossil fuel power plant for heat mining from geothermal reservoirs

Authors

Pan, Chunjian
Romero, Carlos E
Levy, Edward K
et al.

Publication Date

2018-10-01

DOI

10.1016/j.jcou.2018.09.003

Peer reviewed

Fully Coupled Wellbore-Reservoir Simulation of supercritical CO_2 Injection from Fossil fuel power plant for Heat Mining from Geothermal Reservoirs

Chunjian Pan[a], Carlos E. Romero[a], Edward K. Levy[a], Xingchao Wang[a],
Carlos Rubio-Maya[b], Lehua Pan[c]

[a] Energy Research Center, Lehigh University, Bethlehem, PA 18015, USA

[b] Faculty of Mech. Eng., Univ. Michoacana San Nicolás de Hidalgo, Morelia, MC 58030, Mexico

[c] Earth Sciences Division, Lawrence Berkeley Nat. Lab., Univ. of California, Berkeley, CA 94720, USA

Abstract

The concept of injecting supercritical CO_2 (sCO_2) into a geothermal reservoir was computationally investigated to obtain an insight into the performance of such system in terms of the benefit of using CO_2 captured from fossil fuel power plants for geothermal heat mining. A fully coupled wellbore-reservoir system was simulated considering the flow of pure sCO_2 in an injection well, interaction of sCO_2 and water in a permeable reservoir, initially filled with water, and the flow of the two-phase mixture of sCO_2 and water in a production well. A base case simulation was performed. Results of this simulation indicate that this CO_2 application is capable of providing a good source of renewable energy. It was found that for the reservoir section used in this study (0.08 km^3) about 8-9 MW_{th} could be extracted from the geothermal resource in a steady state fashion, for a lifetime of the wells of 30 years. This is approximately equivalent to 100 MW_{th}/km^3. A sensitivity analysis of the coupled wellbore-reservoir system provided information on the impact of certain parameters on the performance of the integrated system. Mass flow rate and temperature of injected CO_2, and reservoir permeability have a first order impact on the pressure management of the reservoir and the amount of heat mining from the CO_2-based geothermal reservoir. Additionally, CO_2 injection temperature has a large effect on the thermosiphon characteristic of this type of systems.

Keywords: Supercritical carbon dioxide, geothermal heat mining, Mexico geothermal power generation.

1. Introduction

The increased concern with rising atmospheric carbon dioxide (CO_2), primarily from anthropogenic fossil fuel combustion, has motivated research and development of alternatives to reduce CO_2 emissions from power and industrial plants. CO_2 capture and sequestration in deep saline aquifers has been considered in a series of studies as a means for controlling this major greenhouse gas. One of the options considers injection of supercritical carbon dioxide (sCO_2) as a working fluid in a naturally high-permeability hydrothermal reservoir [1-4]. In addition to the benefit of sequestering CO_2 in the reservoir, sCO_2 can be used to mine geothermal energy for utilization above the ground. sCO_2, despite having a smaller mass heat capacity than water; under typical geothermal formation underground conditions, has on average 40% of the viscosity of water and a lower density than water. With those properties, injection of sCO_2 would result in an increased mass flow rate across an equivalent geologic reservoir and, additionally, an augmented buoyancy drive. The injected sCO_2 would form a large subsurface CO_2 plume that would permanently sequester CO_2 underground and also absorb heat from the geothermal reservoir for subsequent utilization at the surface, such as enhanced power generation. An artistic illustration of the concept of sCO_2 injection from fossil fuel power plant for heat mining from geothermal reservoirs is presented in Figure 1.

Figure 1: Illustration of sCO_2 Injection into a Geothermal Reservoir for Heat Mining and Above-the-Ground Geothermal Energy Utilization.

This approach is of interest to Mexico, since it combines CO_2 capture and sequestration, geothermal energy extraction and enhanced electric power generation. The Mexican government is committed to reduce its carbon footprint and it has set targets to cut national Green House Gas (GHG) emissions by 22% below baseline in 2030, equivalent to an increase of emissions by 56% above 1990 levels. Mexico releases approximately 709 million tons of CO_2 annually into the atmosphere (the world's 12^{th} largest carbon emitter), with 30% of this inventory coming from the electricity generating sector [5]. It is expected that in a future CO_2-constrained world, relatively pure CO_2 would be available in large quantities from Mexican fossil fuel power plant and other energy intensive industrial facilities, such as chemical process facilities and cement plants. Mexico is conscious of the need to grow its economy, with the associated need to expand its current power generating capacity, and its electricity sector currently heavily relies on fossil energy sources (approximately 75% of the total installed capacity). However, meeting the forecasted future electricity demand with fossil fuels could increase Mexico's CO_2 emissions by 230%. Adoption of green technologies by Mexico, such as solar, wind, hydro, biomass, and geothermal energy is a necessity to significantly mitigate the global warming impact of an increased power generation base. It is recognized that one of the largest renewable energy sources available to Mexico is geothermal energy. The IGA (International Geothermal Association) has reported that Mexico has estimated geothermal reserves of approximately 8,000 MW_e, second in the world only to Indonesia. Mexico has a total of eight geothermal power plants, already installed and in construction, totaling a current installed geothermal capacity of 953 MW_e (fourth in the world) [6]. Additionally, more than 1,000 potential geothermal sites have been identified, with a large concentration of medium- and low-enthalpy reservoirs, encompassing Mexico's volcanic region [7].

The concept of using CO_2 as a working fluid to recover heat from geothermal reservoirs has received a good deal of attention of lately. This as-yet-unproven concept relies on replacing water with sCO_2, which, research results have suggested would be a better working fluid than native reservoir water or brine for geothermal energy extraction [8-17]. Due to its thermofluid behavior under supercritical conditions, a geothermal system utilizing sCO_2 as the subsurface heat exchange fluid, in a naturally porous or fracture permeability-enhanced geologic formation, would provide improved heat extraction for low temperature geothermal resources at shallower subsurfaces below the bedrock. It has been suggested that CO_2-based geothermal systems could operate at up to 1.5 times the electricity-production efficiency of conventional water-based systems [19]. Additionally, the transport and solubility properties of sCO_2 would also help reduce contamination, scaling and degradation of power equipment found in steam-based geothermal systems.

There is a body of literature presenting variations of the application of sCO_2 for heat mining from geothermal resources. The majority of these studies investigate the feasibility of the concept, framing the results on the impact of reservoir nature, properties and geometry on CO_2 plume formation within the reservoir and its associated heat extraction. One of these sCO_2-based concepts consists of injecting CO_2 into dry rock or hydrothermal (wet rock) geological formations, where the CO_2 fracture/fill/displaces the native reservoir fluid, mines geothermal heat and is piped back to the surface for electricity production or other applications. Part of the injected CO_2 can be geologically stored. Brown first [8] presented the use of sCO_2 in hot dry rock reservoirs in 2000. The work by Brown was based on field testing and demonstrations carried out at the Fenton Hill test site in the Jemez Mountains of North-Central New Mexico. The study by Brown concluded that for a 500 m deep hot dry rock reservoir with an injection pressure of 300 bar, about 100,000 tons of CO_2 per year could be sequestered, in addition to about 50,000 tons of CO_2 available for closed-loop circulation.

Pruess [9, 10] presented the concept of CO_2-based Enhanced Geothermal Systems (EGS). In this system, sCO_2 would be injected into the hot impermeable rock; opening additional fractures in the reservoir and forming a region prone for CO_2 diffusion in the reservoir. After initial formation of a two phase CO_2-water mixture in the reservoir, the passage of time will lead to the creation of a reservoir of pure sCO_2, circulating in closed-loop, while extracting heat and sequestering some CO_2 in the surrounding rock mass. In the simulations performed by Pruess [9], a reservoir thickness of 305 m was used, with reservoir rock temperature of 200°C, injection temperature of 20°C, fracture spacing of 50 m, permeable volume fraction 10%, negligible rock permeability and 50 md fracture permeability, 50% porosity in the permeable domain, and variable reservoir pressures. A five-spot well configuration was modelled, with a two-dimensional and five-point grid of 1,000 m side. All simulations were performed using the TOUGH2 [10] code, augmented with the ECO2N fluid property module. All simulations were performed under CO_2-only or H_2O-only systems, with no consideration to mixtures of both fluids, and maintaining the injection and production bottom-well pressures constant. The simulations performed by Pruess [11] conclude that heat extractions from EGS systems can be 50 to 100% larger with sCO_2 than with water. The differences become smaller with time, due to the more rapid thermal depletion when using CO_2. Mass flow rates in the CO_2 system are also larger than for water by factors as high as 3.5. Additional data from the study by Pruess [11] of CO_2-based EGS estimate that typical fluid loss rates (sequestration rates) would be in the range of 5%, further suggesting about 1 kg/sec/MW of sequestered CO_2. Further work by Spycher [12] on EGS systems concluded that the production of a free aqueous phase form in an EGS operated with CO_2 will occur only after a limited number of years. Spycher added that it is typical to expect a useful life of geothermal reservoirs of about 25-30 years.

Randolph [14] introduced the concept of CO_2-Plume Geothermal (CPG) in which sCO_2 is used as the working fluid in a high-permeability, high-porosity geologic reservoir (typically hydrothermal or saline reservoirs) that is overlain by a low-permeability cap rock. The CO_2 displaces the native formation brine in the reservoir, heats up and then is ready for electricity generation at the surface. The sizes of these wet rock reservoirs are typically much larger than those of hydrofractured reservoirs. The simulations performed by Randolph and Saar [14, 15] are an extension of the work by Pruess [9] in which the same five-well arrangement and geometry was used and resolved using the TOUGH2 code with the ECO2N fluid property module. Different values of domain permeability were tried by Randolph, with an average value of $5x10^{-14}$ m^2. Other simulation parameters include a 20% domain porosity, reservoir pressure of 250 bar, and two reservoir assumed depths and corresponding temperatures of 4 km-150°C and 1 km- 100°C. Heat extraction rates estimated by Randolph for a 25-year average were of 62.6 MW for the deep reservoir and 64.1 MW for the shallow reservoir. The results for the CPG systems show that the heat extraction decreases with time as the heat is depleted and the temperature at the production wells decreases with time. The work of Randolph also compares CPG CO_2-based systems vs. CPG H_2O-based systems. Cases run at different combinations of initial reservoir pressure and temperature show that for an average 25-year reservoir lifetime, the heat extraction rates for CO_2 are between 2.3 to 3.0 times larger than for the H_2O-based cases. The corresponding heat extraction ratios of CO_2 to H_2O are in the range from 4.9 to 5.5 [14, 15].

Additional references have reported studies on CO_2 utilization for heat mining considering the geothermal reservoir only. Salimi and Wolf [16] presented another concept for CO_2 utilization in geothermal sites. This concept involves co-injection of CO_2 and water, to prevent drying out and over-pressurizing the reservoirs. Another advantage of this concept is related to the dissolved phase of CO_2 in water, which would avoid confinement of CO_2 to the upper part of the reservoir, decreasing leakage via the cap rock. Self-developed model results were presented that indicate that at CO_2 mole fractions below 0.10, cumulative heat extraction from such system can be as high as 1,000 TJ for 30 years, for a reservoir with dimensions of 250 m thick, 1,600 m long, mean porosity of 0.17, permeability of 21.6 mD and initial temperature of 80°C. Buschneck et al. [17] introduced a hybrid two-stage approach to sequester CO_2 and produce geothermal energy in saline, sedimentary formations. In this concept, first brine is extracted from the reservoir to provide pressure relief for CO_2 injection; then, when CO_2 is injected and it reaches the production wells, co-produced treated brine and CO_2 become the working fluids for energy recovery. Three-dimensional model results, using the NUFT code, for reservoirs with temperatures in the 100°C range, report heat extraction rates with this approach as large as 100 MW/m^2, with combined production flow rates as high as 280 kg/s. A recent study presented by Zhang, et al [18], confirms that sCO_2 has good mobility and heat capacity, and it can be used as an alternative to water for heat recovery from geothermal reservoirs. In the work of Zhang, et al [18] different types of geothermal resources for China were assessed to screen reservoirs suitable for heat mining and geological storage by CO_2 injection, in terms of geological properties, heat characteristics, storage applicability, and development prospects. Reservoir simulations were conducted to analyze the heat extracting capacity and storage efficiency of CO_2 using a simple calculation method. The assessment results show that the recoverable geothermal potential by CO_2 injection in China is around $1.55x10^{21}$ J, using Hot Dry Rock (HDR) as the main geothermal resource contributor. The corresponding CO_2 storage capacity is up to $3.53x10^{14}$ kg with the deep saline aquifers accounting for more than 50% of total. It was concluded in this study that CO_2 injection for geothermal production is a more attractive option than pure CO_2 storage due to its higher economic benefits in spite of that many technological and economic issues still need to be solved. Finally, a study by the authors of this paper [19] reports an assessment of the feasibility of using sCO_2 for heat mining for twenty-one geothermal sites in Mexico. This represents the totality of fully characterized geothermal sites in Mexico. The power generation estimate for all the sites is of the order of 1,160 MW_e, representing a 51.4% additional power generation with sCO_2 than with water. Additionally, it was found from the work reported in Reference 18 that the sum of the Mexican sCO_2-based systems would be able to sequester, over an expected 30-year life of the reservoirs, approximately 72 million tons of CO_2. Simulations were carried out using the TOUGH2 code, while neglecting the wellbore flows, and with the evaluation of the CO_2 or water heat mining performance, exclusively depending on reservoir properties and behavior.

This paper reports results of a study focused on exploring the injection of CO_2 from fossil fuel power plant for heat mining from geothermal reservoirs in a fully coupled wellbore-reservoir system. The system was simulated in an integrated fashion that considers the flow of pure sCO_2 in an injection well, interaction of sCO_2 and water in a permeable reservoir, initially filled with water, and the flow of the two-phase mixture of sCO_2 and water in a production well. A research version of the T2Well/ECO2N software was used in the simulations. A symmetry section of a five-spot well arrangement was modeled, using a 3-D orthogonal coordinate system. Reservoir properties, fluid flow conditions and well arrangement representative of similar systems in Mexico and of the CO_2 sequestration industry were used in the simulations. The results provide an insight into the behavior of the coupled wellbore-reservoir configuration for the CO_2/water mixture. A parametric analysis, performed with the integrated model, also provides an indication of a strategy for management of the heat mining process.

2. Modeling Approach

2.1 Conceptual Model and Gridding

The coupled wellbore-geothermal reservoir model considered in this study is showed in Figures 2 and 3. The model is a symmetrical box of the five-spot well configuration pattern [9]. For the production wells at the edges of the modeling domain (Figure 3), it is assumed there are hard rock boundaries, so zero flux boundaries were applied. For the box computational domain in the middle, zero flux boundaries were applied due to symmetrical flow pattern. Researchers have reported modeling results for half of the box shown in Figure 3, divided by the diagonal line between the injection and production wellbores [9, 20]. Thus, only 1/8 of the basic configuration pattern is considered in the model domain. In this study, a 1/4 model of the basic pattern and the wellbore was modeled. By modeling a box, the default mesh generator in the solution solver used in this study was able to be applied directly.

The base case dimensions are shown in Table 1 (see also Figure 2). Reservoir characteristic parameters for the base case simulation are shown in Table 2. The general reservoir parameters were based on measured data from some typical reservoirs in Mexico [19]. Initial reservoir conditions as well as injection conditions are included in Table 3, where the initial pressure is increased by 10 bar for every 100 m of depth. The heat and mass flux were both assumed to be zero on all reservoir boundaries. Injection wellhead conditions were set at 30 kg/s, 35°C. Production wellhead conditions were set at 200 bar. Along the length of the wellbore on top of the reservoir, a linear temperature distribution was assumed, ranging from 35 to 225°C.

A mesh grid of 30×30 cells along the horizontal direction was used, with a finer mesh used near the two wellbores. The depth of the reservoir was equally discretized into 10 layers. This mesh sizing is quite typical for reservoir discretization. For the wellbores, equal cell length of 50 m was used, resulting in 30 cells for the wellbore part above the reservoir. Together there are 9,060 cells.

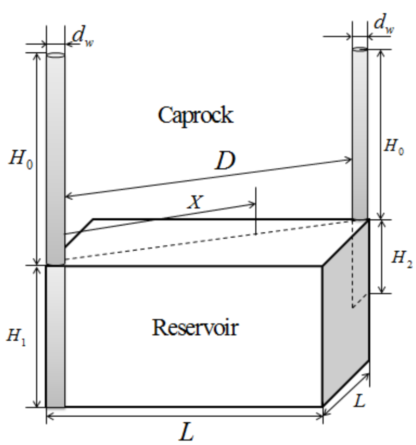

Figure 2. Diagram of Coupled Wellbores and Reservoir (see Variable Definition in Table 1)

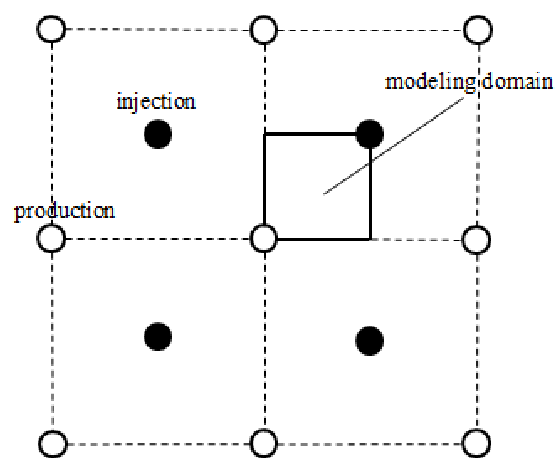

Figure 3. Plane View of the Five-Spot Well Pattern

Table 1. Model Dimensions

Wellbore Length Through the Caprock Portion, H_0

Injection Wellbore Depth in the Reservoir Portion, H_1
Production Wellbore Depth in the Reservoir Portion, H_2
Length of Reservoir Side, L
Diameter of Injection and Production Wellbores, d_w
Diagonal Distance Between the Injection and Production Wellbore , D
Coordinate or Diagonal Distance with Origin at the Injection Well, X

Table 2. Reservoir Characteristic Parameters

Permeability	30 mD
Porosity	0.1
Rock grain density	2600 kg/m^3
Rock specific heat	920 J/(kg*°C)
Rock thermal conductivity	2.51 W/(m*°C)
Parameters for Relative Permeability [20] Residual Gas Saturation m_{VG} Residual Liquid Saturation Saturated Liquid Saturation	 0.01 0.65 0.05 1.00
Parameters for Capillary Pressure [20] Residual Liquid Saturation m_{VG} Alpha Maximum Capillary Pressure Saturated Liquid Saturation	 0.03 0.4118 6.06E-5 Pa^{-1} 6.40E+7 Pa 1.00

Table 3. Initial Reservoir and Injection Conditions

Reservoir fluid	All water	Injection fluid	CO_2
Initial Temperature	225°C	Injection temperature	35°C
Initial Pressure	150-200 bar	Injection mass flowrate	30 kg/s

2.2 Simulator

The fully coupled wellbore-reservoir simulator T2Well was used in this study. Detailed mathematical descriptions and validations of T2Well are available in [21-24]. This software is commercially available for temperatures up to 100°C. A high temperature research version, provided by Lawrence Berkeley National Laboratory, was used in this study, which is capable to provide CO_2-brine mixture property values up to 300°C . T2Well incorporates the widely used reservoir-simulation code, TOUGH2 [10]. The equation of state model used was the ECO2N V2.0 [25], which includes a comprehensive description of the thermodynamic and thermo-physical properties of the H_2O-NaCl-CO_2 system in the pressure and temperature ranges for typical geothermal systems. In T2Well, the wellbore and reservoir are two different subdomains where flow is controlled by different physics. Specifically, viscous flow in the wellbore is governed by the 1-D momentum equation, while 3-D flow in the porous reservoir is governed by a multiphase version of the Darcy's Law. The mass and energy balances are solved together for the two domains, thus capturing the coupled behavior between a wellbore and a reservoir.

3. Results and Discussion

3.1 Base Case

This section presents simulation results for the base case. Figure 4 shows the pressure behavior in the reservoir at different distances, on a diagonal, from the injection to the production well. Simulations were run for a period of 30 years. The pressure traces in Figure 4 correspond to results obtained from the simulations for the top discretized layer beneath the caprock in the reservoir. Initially, the pressure in the reservoir quickly increases over the entire reservoir from the initially 150-200 bar to reach a peak around 445 bar. Then the pressure in the reservoir gradually decreases as the gas phase breakthrough the production well (Figure 5). Also a large pressure gradient in the reservoir around the production wellbore can be observed, as indicated by the bottom two pressure traces in Figure 4. The pressure at the production wellhead was set at 200 bar (this boundary condition may be too high during the water production period in a real case; although, this pressure level would be more realistic for a CO_2 breakthrough), and during the first few years, when the production flow is mostly pure liquid water, the production mass flowrate of the liquid phase goes up to 50 kg/s, and then it drastically decreases to reach a steady flowrate of the order of 30 kg/s (close to the injection flow rate). At the steady production flow conditions, more than 80% of the flow mass fraction is CO_2, as shown in Figure 5. The CO_2 mass fraction is the flowing fraction (i.e., the ratio of CO_2 mass flow rate over the total mass flow rate. However, during the first few years of injection, there is a pressure buildup in the reservoir due to the large mass flowrate of cold CO_2 being heated in the reservoir. This leads to a large CO_2 compression inside the reservoir, faster than the available reservoir volume can be emptied by the amount of water leaving the reservoir. Pressure spikes inside the reservoir are not desirable since they increase the risk of caprock fracture and potential CO_2 leakage to the surface.

When the production is CO_2 dominated, the compression effect is greatly reduced, the pressure peak disappears and the flowrate in the production well reaches steady state. This pressure peak behavior is quite unique for CO_2 injection in a reservoir initially filled with water, which will not happen if the reservoir would be initially filled with CO_2. In a real application, there would be limitations in compressor work that would prevent injection of CO_2 at the target 30 kg/s for the reservoir characteristics used in this study. Strategies would need to be developed to prevent the pressure peak from occurring; i.e., during the first few years of CO_2 injection, a smaller CO_2 injection flowrate could be used, until the CO_2 plume fully develops and CO_2 production dominates in the production well. Another option would be to open the production wellhead to a lower pressure. Then the injection rate could be increased to larger values. Other possible option would be to add reservoir pressure relief through water or brine production wells. This option has been suggested in other references [17], with further reference to water/brine utilization in other production processes, like desalination.

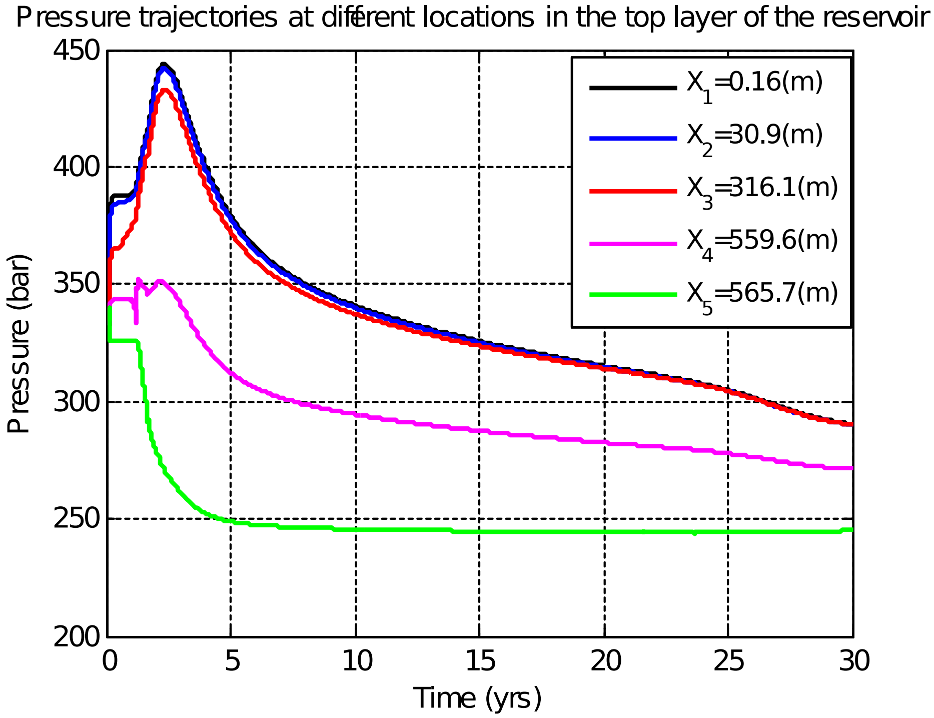

Figure 4. Pressure Traces in the Top Layer of the Reservoir

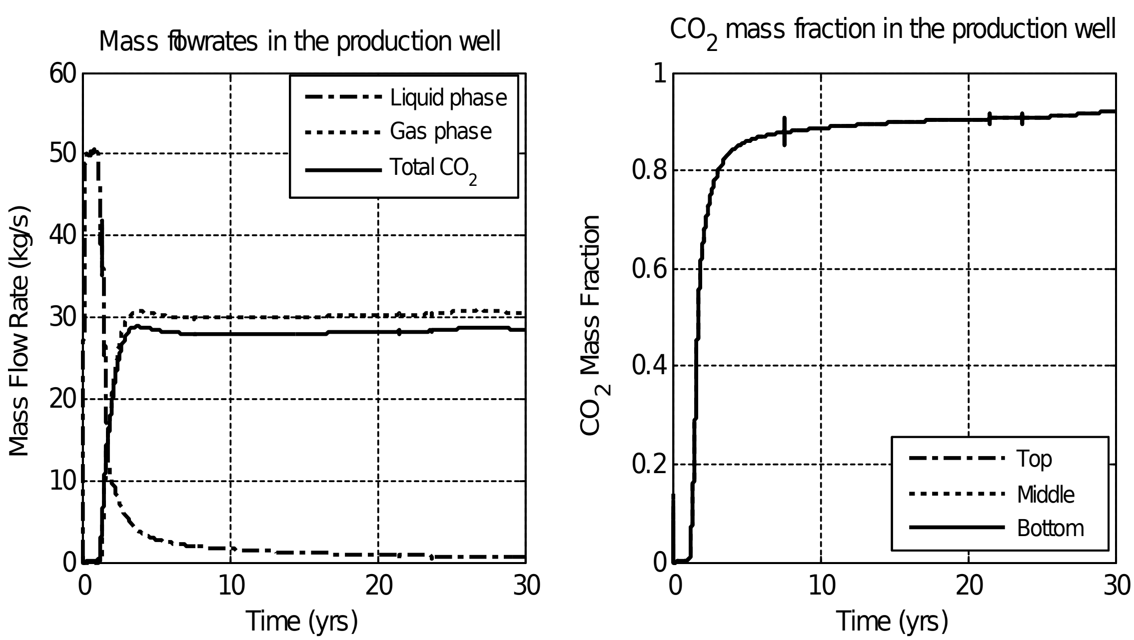

Figure 5. Mass Flowrates (left) and CO_2 Mass Fraction (right) in the Production Well

Figure 6 shows pressures at the injection and production wellhead and well bottom, as well as the pressure gain or loss in the wells and reservoir. Injection pressure gain is defined as the pressure differential from injection wellhead to well bottom. Production well pressure loss is defined as the pressure differential from production well bottom to wellhead, while reservoir pressure loss is defined as the change in pressure in the reservoir from injection well bottom to production well bottom. It can be seen in Figure 6 that the pressure peak in the reservoir is reflected in the pressure trace at the injection wellhead. The density difference between the injection well and the production well is the main cause for the development of the thermosiphon phenomenon in which the injection wellhead pressure is lower than the production wellhead pressure. As shown in Figure 6, this happens after about 13 years when the pressure loss through the reservoir significantly drops because of well development of CO_2 plume in the reservoir.

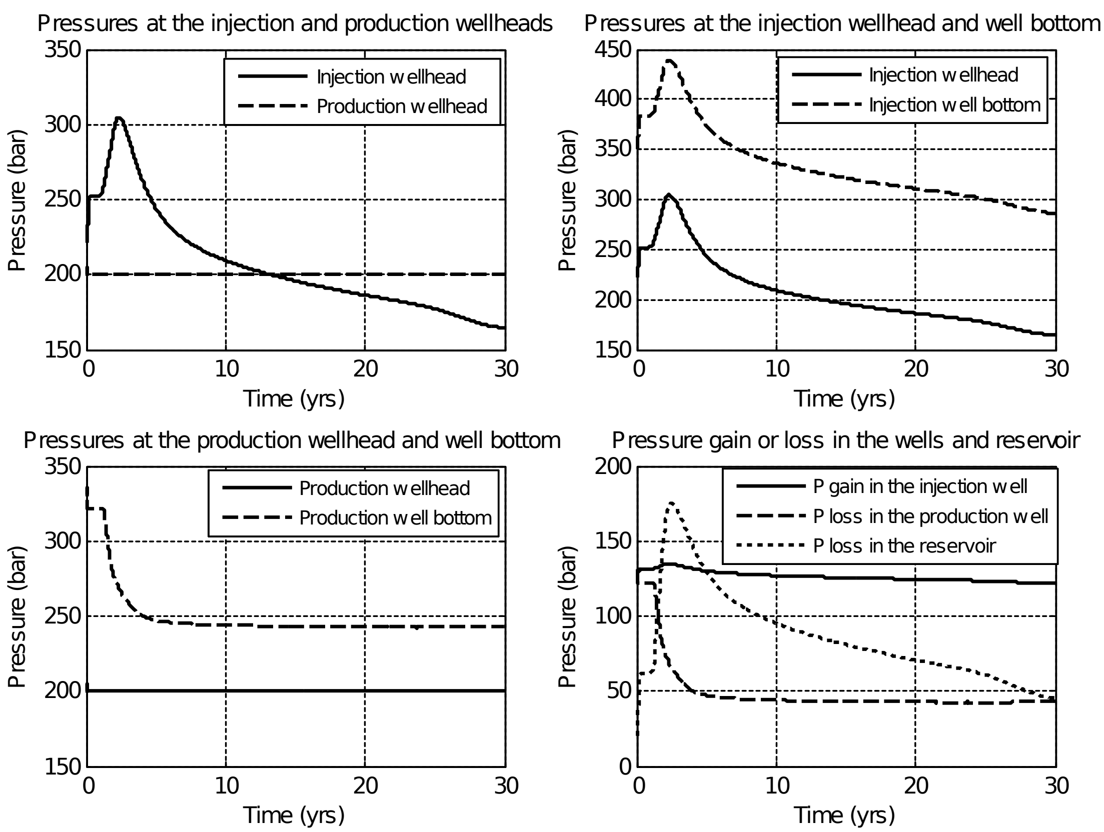

Figure 6. Pressures in Injection and Production Wells

Figure 7 shows temperature plots at the production wellhead and bottom. The temperature drop between these two locations is almost constant from well bottom to head when the production is CO_2 dominated. At about 26 years after the start of injection, the temperature in the reservoir begins to drop and the output temperature at the production wellhead begins to decline. This provides an indication that an optimal well configuration and heat mining strategy are required to exploit geothermal resources with CO_2 in a cost-efficient manner. Figure 8 shows the net energy flow produced from the reservoir. The energy flow is based on the following calculation:

$$\dot{Q}=\dot{m}_{pro}^{CO_2}h\left(P_{pro},T_{pro}\right)-\dot{m}_{inj}^{CO_2}h\left(P_{inj},T_{inj}\right) \qquad (3.1)$$

where $\dot{Q}$ is the energy flow from the production well hot stream, $\dot{m}_{inj}^{CO_2}$ is the injected CO_2 mass flowrate, $h\left(P_{inj},T_{inj}\right)$ is CO_2 enthalpy at the injection wellhead, $\dot{m}_{pro}^{CO_2}$ is the pure CO_2 mass flow rate at the production well, and $h\left(P_{pro},T_{pro}\right)$ is CO_2 enthalpy at the production wellhead. The fluid generated at the production well will be a rich CO_2 mixture with some entrained water, with a steady state mass fraction of water of less than 10%. The MW calculation assumes that water is separated before further CO_2 heat utilization. It is estimated that for the reservoir used in this study, about 8-9 MW_{th} could be extracted from the geothermal resource for a reservoir section with a volume of 0.08 km^3, or an approximate equivalent 100 MW_{th}/km^3. During the first two years, the net energy flow is less than zero; this is because there is almost no CO_2 production during the beginning years, while the hot water being produced was not considered to be used to produce energy. For the base case, the total amount of CO_2 being sequestrated in the 30-year time lapse is 3.3 Mt in the box domain, or 41.2 kg/m^3. The total amount of water being extracted was 5.4 Mt, or 68.1 kg/m^3. As the density of water is heavier, more water was extracted.

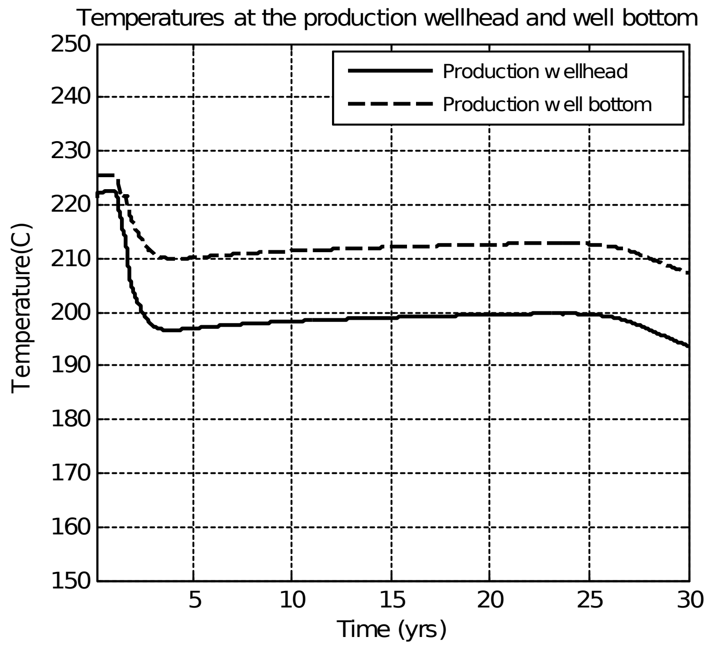

Figure 7. Temperatures at the Production Wellhead and Well Bottom

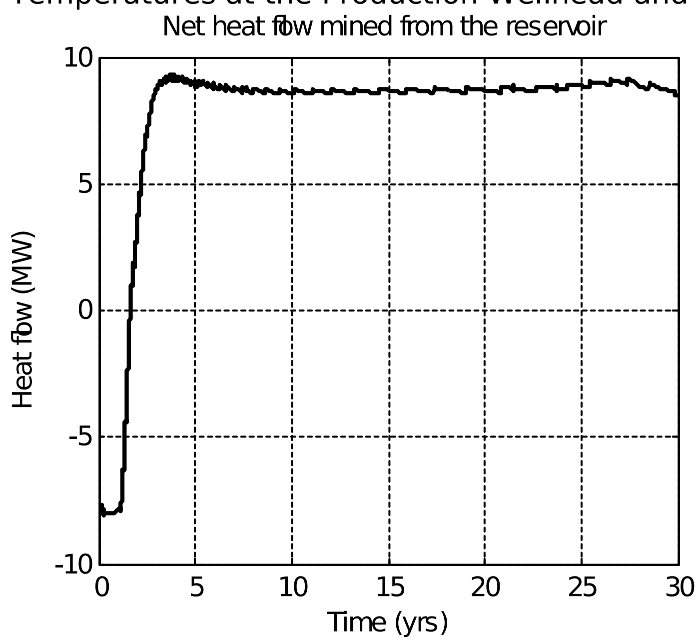

Figure 8. Net Power produced from the Reservoir

Figures 9 to 11 show contours of pressure, temperature and CO_2 saturation in a diagonal vertical plane between the two wellbores. Results are presented for 1, 5, 15 and 30 years. The highest pressure in the reservoir is located at the injection well bottom, while the lowest pressure is located at the production well bottom. The overall the pressure level in the reservoir decreases throughout the 30-year period. From Figure 10, it can be seen that the temperature in the reservoir drops after 30 years. This is consistent with the contours of Figure 11, which show the gradual propagation of CO_2 inside the modeling domain. Figure 11 shows that CO_2 concentrates at the bottom of the reservoir, propagating from the injection to the production well bottom, which is also consistent with pressure gradients shown in Figure 9. In this study it was found that this CO_2 behavior greatly depends on the permeability of the reservoir (The CO2 plume would stay at the top of the reservoir if the reservoir permeability was 15mD.). Figure 11 also shows that by Year 30, the CO_2 gas plume has diffused to almost occupy the entire reservoir volume. It should be noted that the CO_2 saturation values in close to the production well bottom are impacted by the resolution in the computational results achieved by the model grid size. The results in Figure 11 also suggest that well arrangement, in this CO_2 utilization application, would be subject of optimization, in order to provide for a system that supplies consistent geothermal energy for the life of the wells. The well arrangement should also be subject to constraints oriented to prevent reservoir over-pressurization and rapid achievement of CO_2 purity and maximum achievable temperature at the production wellhead.

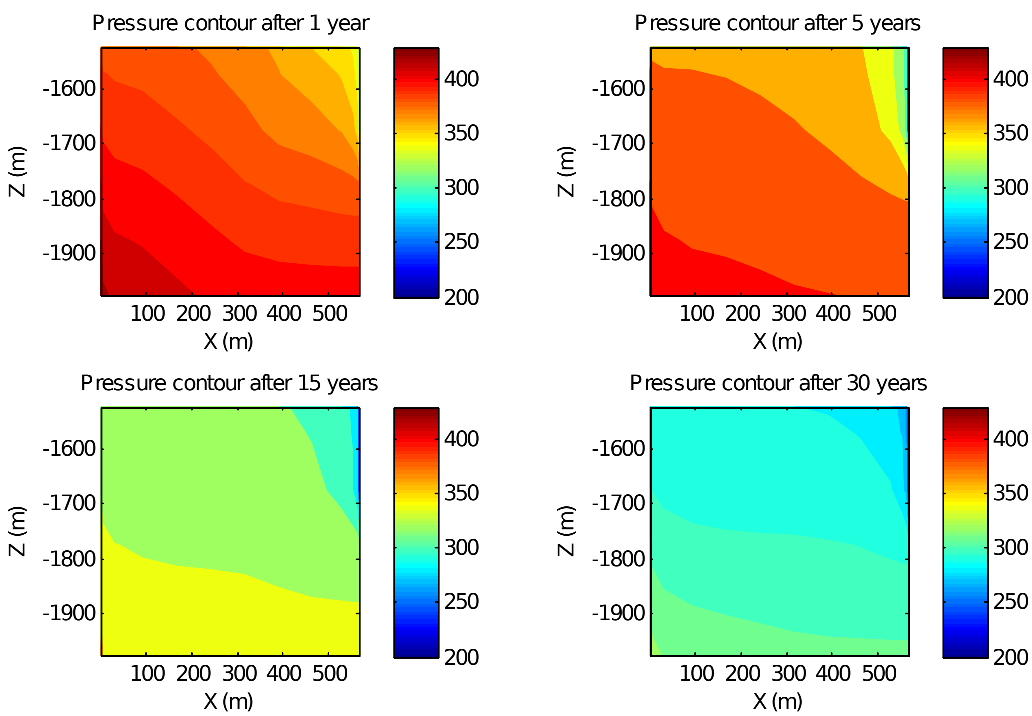

Figure 9. Pressure Contours at the Vertical Diagonal Plane between the two wellbores

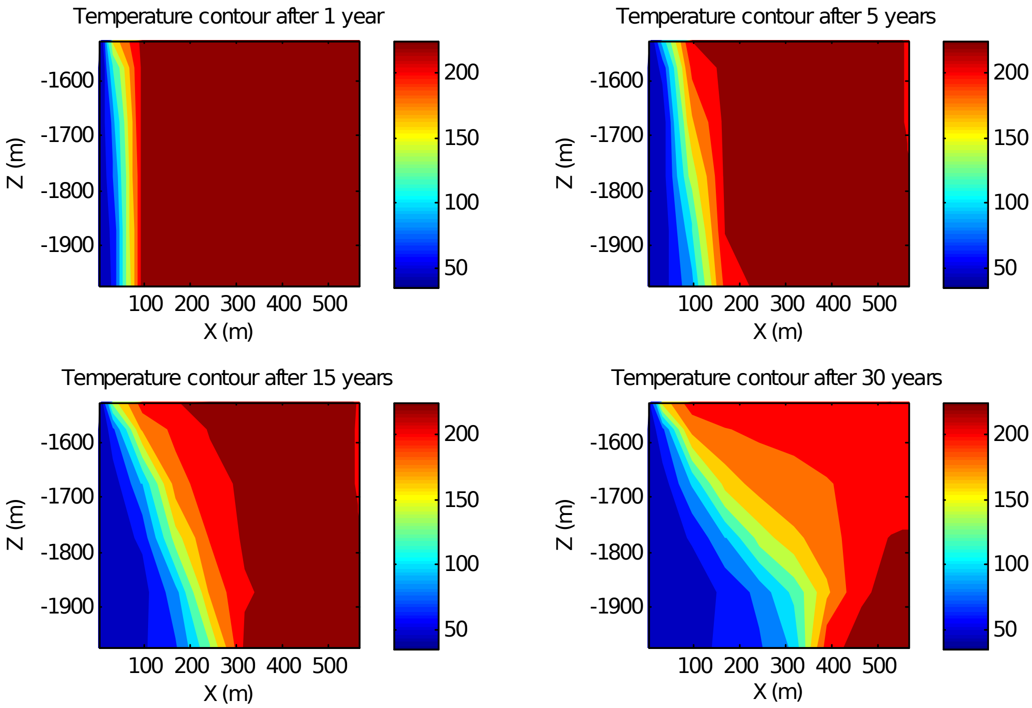

Figure 10. Temperature Contours at the Vertical Diagonal Plane between the two wellbores

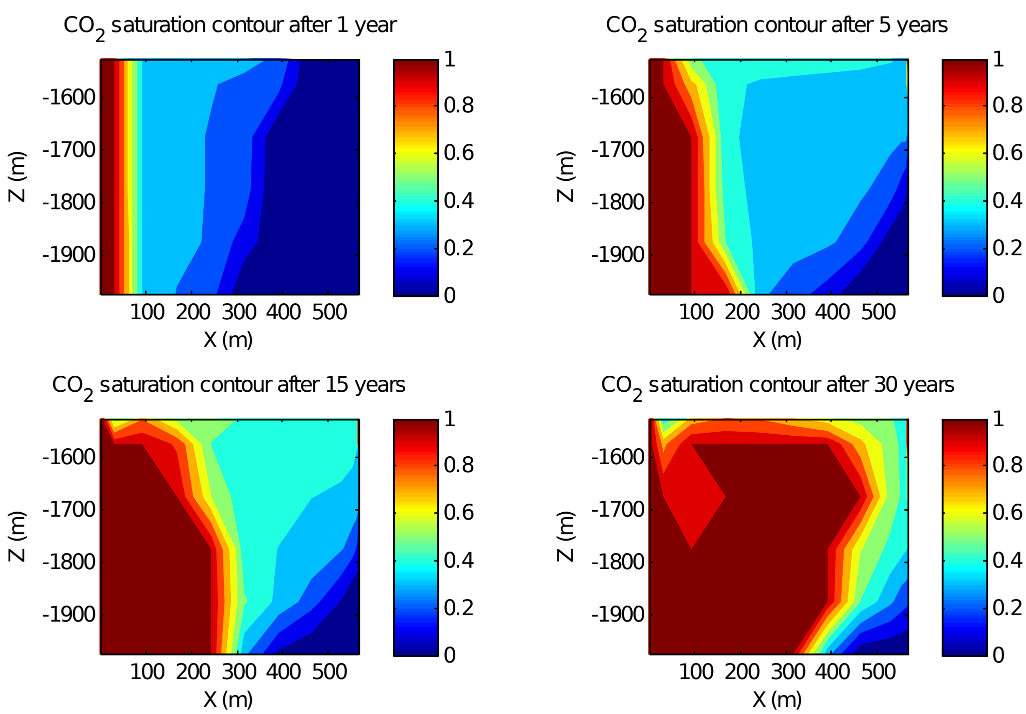

Figure 11. CO_2 saturation Contours at the Vertical Diagonal Plane between the two wellbores

3.2 Sensitivity Analysis

A sensitivity analysis of seven input parameters used in the simulation was performed (see Table 4). Figure 12 shows results of the sensitivity analysis corresponding to variations of the pressure specified in the model formulation at the production wellhead boundary condition. Results are presented in terms of the pressure differential between the injection and production wellhead, CO_2 production temperature, net energy flow (see definition in Section 3.1 Eqn. 3.1) and CO_2 mass fraction (see Figure 12). The specified pressure at the production wellhead has little impact on the thermosiphon effect (production pressure larger than injection pressure) of CO_2 utilization in geothermal reservoirs. Similarly, the impact of the production pressure is negligible on the net energy flow (this is expected because the CO_2 injection rate is fixed) and production stream CO_2 mass fraction. However, the impact of the specified pressure at the production wellhead on the output temperature at the production wellhead is significant. The higher the production pressure, the higher the production temperature. This is mainly because CO_2 is compressible fluid so that the temperature is proportional to the pressure for the same given specific enthalpy.

Table 4. Parameters for Sensitivity Analysis

#1	Specified pressure at the production wellhead, P_{Pro}
#2	CO_2 injection temperature, T_{inj}
#3	Reservoir permeability, Pm
#4	Injection flowrate, F_{inj}
#5	Reservoir length, L
#6	Extension depth of the production wellbore into the reservoir, H_2
#7	Diameter of the production wellbore, d_w

Figure 13 shows sensitivity analysis results for injection of CO_2 at temperatures from 35℃ to 75℃. The output temperature at the production wellhead and corresponding CO_2 mass fraction at the production well are all unaffected by the changes in injection temperature over this range. The thermosiphon effect is slightly affected by this change in injection temperature, because the colder CO_2 has larger density which results in less injection wellhead pressure needed to maintain the same injection well bottom pressure to drive the CO_2 through the reservoir to the production well whose wellhead pressure is fixed. This effect was already reported by Reference 19. However, it should be noticed that at the 75℃ injection temperature, the thermosiphon effect appears only when close to the end of 30 year operation. It was also found that a higher injection temperature would lead to a lower net energy flow. This is mainly because of higher CO_2 enthalpy at a higher injection temperature.

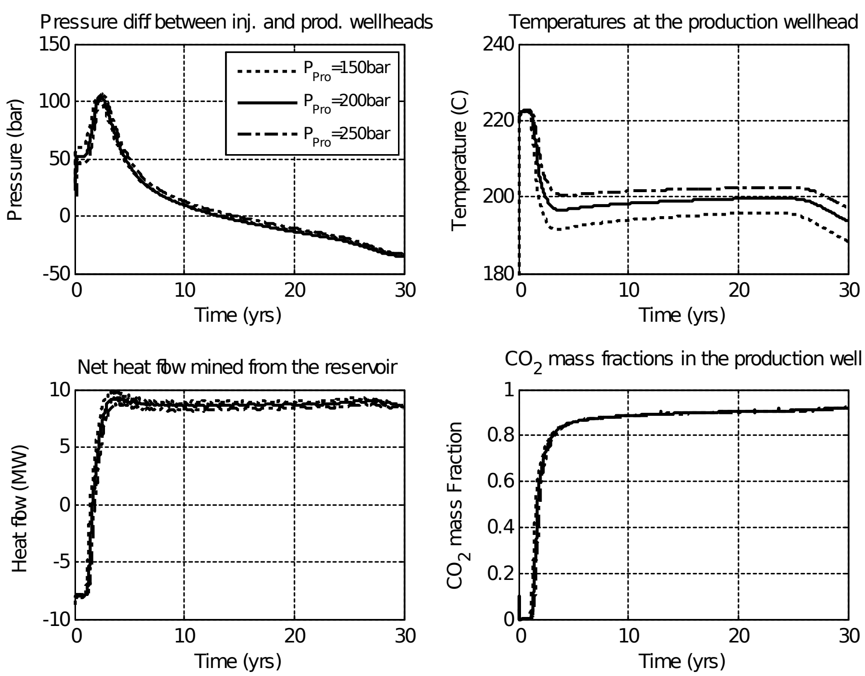

Figure 12. Sensitivity Analysis Results for Specified Pressure at the Production Wellhead

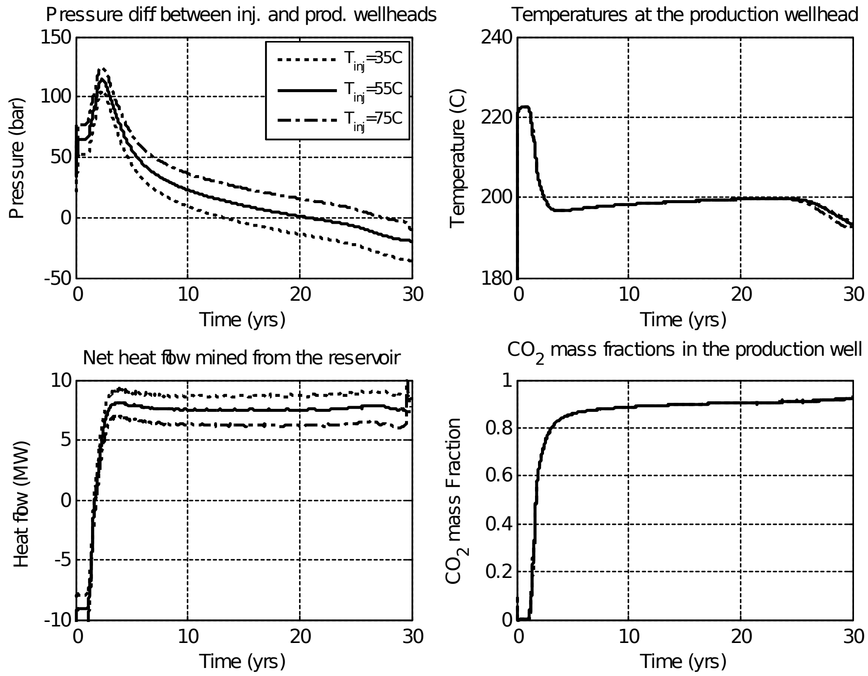

Figure 13. Sensitivity Analysis Results for Different Injection Temperature

Figure 14 shows sensitivity analysis results corresponding to different reservoir permeabilities. A range of permeabilities between 15 to 50 mD was used in the simulations. The reservoir permeability has a great impact on the pressure spike seen in previous results at the beginning of CO_2 plume formation. The pressure peak almost disappears when the permeability is 50md. Additionally, it was found that when the reservoir permeability is large, higher output temperatures (with the same production pressure) can be achieved the production wellhead. However, the impact of reservoir permeability on net energy flow is negligible because of the small enthalpy variation of CO_2 around $200℃$. Figure 15 shows the impact of injection flowrate on the parameters of interest. It can be seen from Figure 15 that there is a relationship between injection flowrate of CO_2 and the magnitude of the pressure spike in the reservoir, further indicating that for certain reservoir characteristics and dimensions, there may be a maximum injection flowrate below which prevention of pressure spikes is possible. As expected, the CO_2 injection flow rate directly controls the production flow rate since a stable injection-production state is established after a few years of injection (see Figure 5); thus, resulting in a steady net production energy flow. However, larger injection flow rates could result in a faster depletion of the geothermal energy reserve in the reservoir.

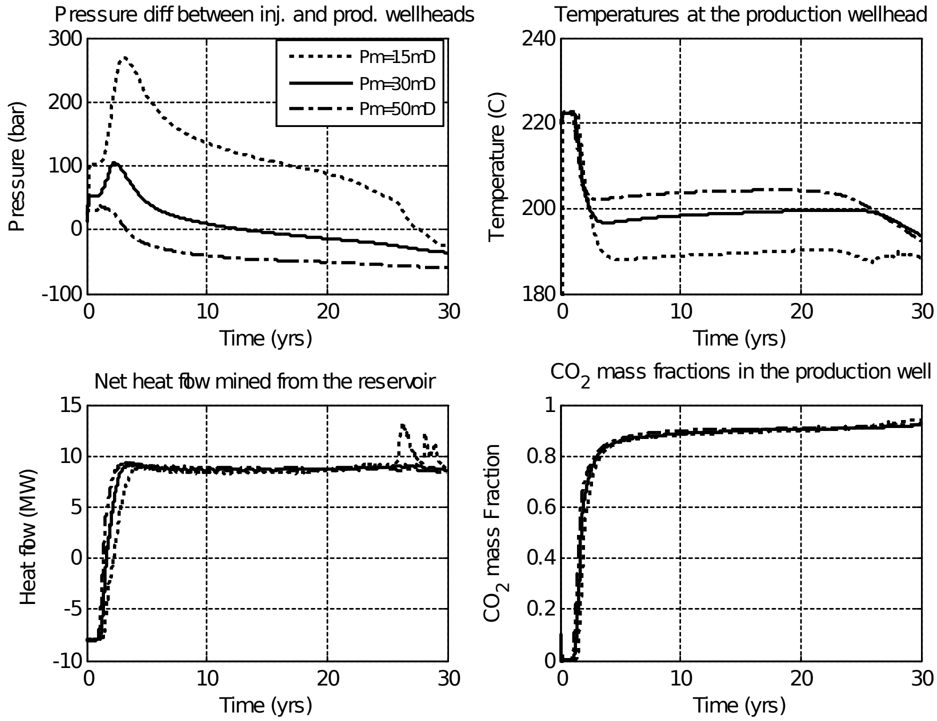

Figure 14. Sensitivity Analysis Results for Different Reservoir Permeability

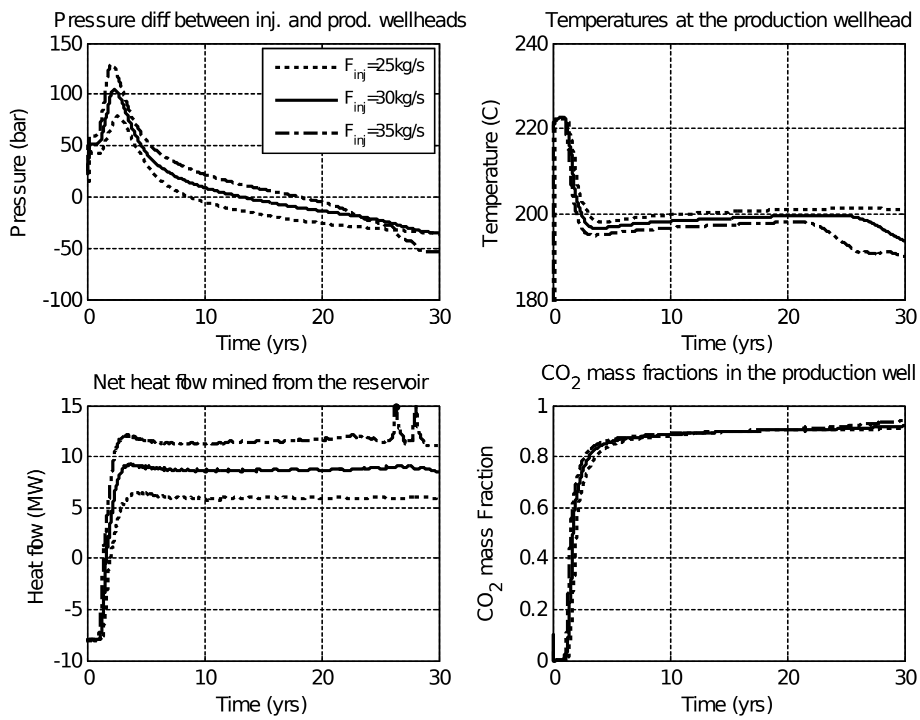

Figure 15. Sensitivity Analysis Results for Different Injection Flowrate

Figures 16 to 18 show sensitivity analysis results as function of production well dimensions and configuration. It can be seen from Figure 16 that larger distances between the locations of the injection and production wells will ensure that the output temperature at the production wellhead will not decline toward the end of the site production life for the same injection flowrate of 30 kg/s. A larger well spacing also contributes to a smaller peak of reservoir pressure. These are all because the larger well spacing means larger capacity of the reservoir involved. As expected, the impact of the distance between both injection and production wells has a negligible impact of produced net energy flow and mass fraction except the early transient period. Figure 17 shows sensitivity analysis results on the impact of extending the depth of the production wellbore into the reservoir. A shallower production wellbore resulting in larger initial pressure spikes because of its smaller well-reservoir interface area (i.e., larger resistance to flow. The impact of this parameter on the produced CO_2 conditions (net energy flow, CO_2 mass fraction and production temperature) is negligible. It is important to notice that the estimation of the effect of the arrangement of the wellbore in the reservoirs would not be possible without a simulation like the one of this study, which couples the wellbores and reservoir in an integrated fashion. Lastly, Figure 18 shows the impact of the production wellbore diameter on performance parameters. In the figures, a larger bore diameter has twice the section area than a smaller diameter wellbore. It was found that this parameter plays no significant role in the operation of the integrated system with fixed production pressure and fixed injection rate, except the pressure difference between injection and production wells.

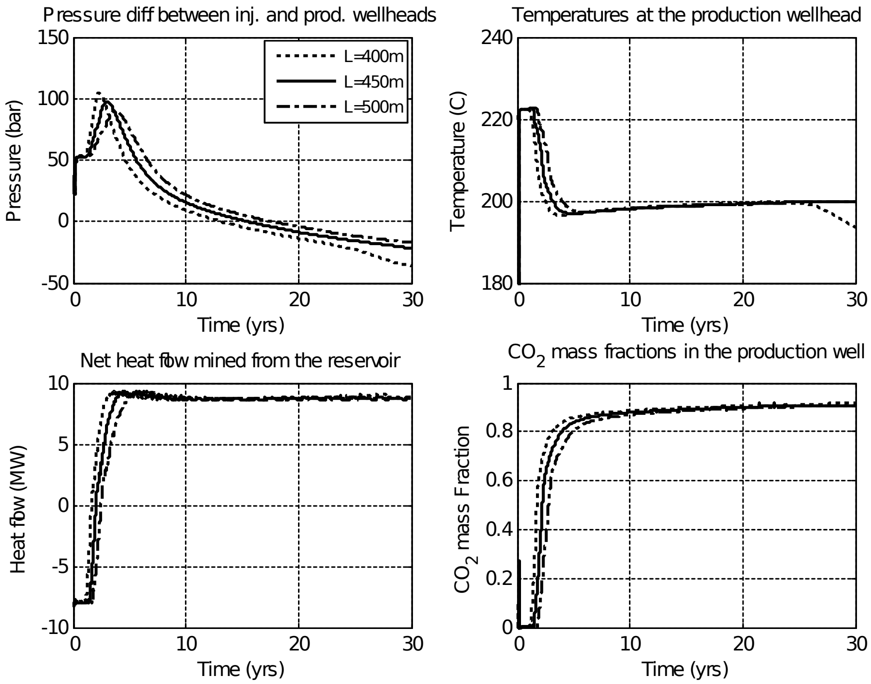

Figure 16. Sensitivity Analysis Results for Different Distance Between Injection and Production Wells

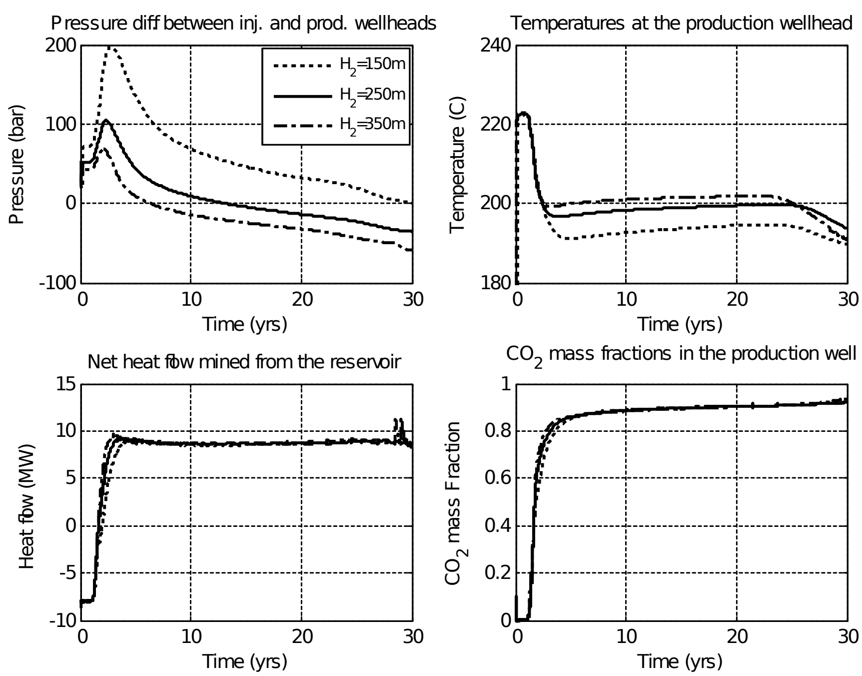

Figure 17. Sensitivity Analysis Results for Different Extension Depth of the Production Wellbore into Reservoir

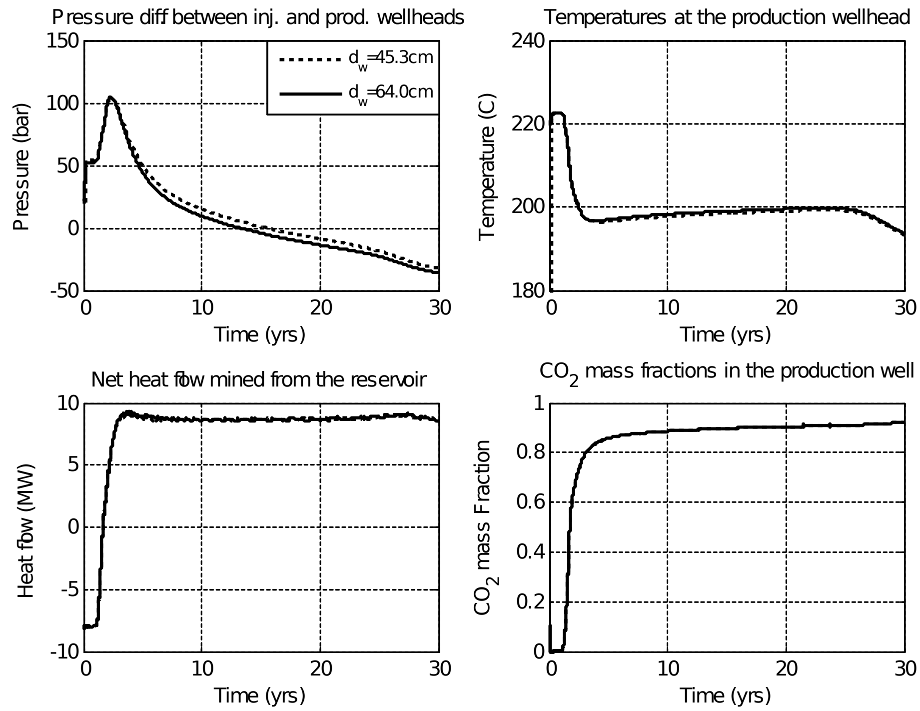

Figure 18. Sensitivity Analysis Results for Radius of the Production Wellbore

4. Conclusions

The concept of injecting sCO_2 into a geothermal reservoir was investigated computationally to obtain an insight into the performance of such system in terms of the benefit of using CO_2 captured from fossil fuel power plants for geothermal heat mining. This approach is of interest to Mexico, since it combines CO_2 capture and sequestration, geothermal energy extraction and enhanced electric power generation. The Mexican government is committed to reduce its carbon footprint and it has set targets to cut national GHG emissions by 22% below baseline in 2030. A fully coupled wellbore-reservoir system was simulated using a research version of the Lawrence Berkeley National Laboratory's T2Well/ECO2N software. The system was simulated in an integrated fashion, considering the flow of pure sCO_2 in an injection well, interaction of sCO_2 and water in a permeable reservoir, initially filled with water, and the flow of the two-phase mixture of sCO_2 and water in a production well. Reservoir properties, fluid flow conditions and well arrangement representative of similar systems in Mexico and of the CO_2 sequestration industry were used in the simulations.

A base case simulation was first performed. Results of this simulation indicate that, despite a pressure peak that can develop during the initial stage of CO_2 injection, this CO_2 application is capable of providing a good source of renewable energy. It was found that for the reservoir section used in this study (0.08 km^3) about 8-9 MW_{th} could be extracted from the geothermal resource in a steady state fashion, for a lifetime of the wells of 30 years. This is approximately equivalent to 100 MW_{th}/km^3. A sensitivity analysis of the coupled wellbore-reservoir system provided information on the impact of certain parameters, such as injection flow rate and temperature, and well configuration on the performance of the integrated system. It is found that the mass flow rate and temperature of injected CO_2, and reservoir permeability have a first order impact on the pressure management of the reservoir. Injection flow rate and temperature have additional impact on the amount of heat mining from the CO_2-based geothermal reservoir. Additionally, CO_2 injection temperature has a large effect on the thermosiphon characteristic of this type of systems, where the pressure differential between production and injection wellhead pressure is positive. From the sensitivity analysis it was evident that system optimization is warranted on these integrated wellbore-reservoir arrangements, to provide a set of optimal operating conditions and well configuration that will result in a cost-effective geothermal resource exploitation.

5. Acknowledgements

This study was funded by the Mexican National Council of Science and Technology (CONACYT in Spanish), under the Sectorial Fund for Energy Sustainability, CONACYT-Secretary of Energy (No. S0019-2012-04). The team formed by the Lehigh University Energy Research Center and the University Michoacana de San Nicolás Hidalgo, are grateful to the administrators of the Mexican Center for Innovation in Energy-Geothermal (CEMIE-Geo in Spanish) for their support and administration of the program. Additionally, the team is grateful to The University of California, Berkeley, for providing his research version of the T2Well\ECO2N v.2 code for high temperature simulations.

6. References

1. Randolph, J. and Saar, M., “Coupling Carbon Dioxide Sequestration with Geothermal Energy Capture in Naturally Permeable, Porous Geologic Formation: Implications for CO_2 Sequestration,” Energy Procedia, 4, 2206-2213, 2011.
2. Buscheck, T., et al., “Multi-Fluid Geothermal Energy Production and Storage in Stratigraphic Reservoirs,” Geothermal Research Council Transactions, 37, 2013.
3. Kervevan, C., et al., “CO_2-DISSOLVED: a Novel Concept Coupling Geological Storage of Dissolved CO_2 and Geothermal Heeat Recovery – Part 1: Assessment of the Integration fo an Innovative Low-Cost, Water Based CO_2 Capture Technology,” Energy Procedia, 2013.
4. Garapati, N., et al., “Total Heat Energy Output form, Thermal Energy Contributions to, and Reservoir Development of CO_2 Plume Geothermal (CPG) Systems,” Proceedings Thirty-Ninth Workshop of Geothermal Reservoir Engineering, Stanford University, California, 2014.
5. Commission for Environmental Cooperation, http://www.cec.org/files/PDF/POLLUTANTS/MXHg-air-maps_en.pdf, [accessed January 2014].
6. International Energy Agency Geothermal Energy Homepage, http://www.iea.gia.org, [accessed December 2013].
7. U.S. Energy Information Administration. EIA, Mexico's Key Energy Statistics, 2012. http://www.eia.gov/beta/international/country.cfm?iso¼MEX [accessed January 2014].
8. Brown, D., “A Hot Dry Rock Geothermal Concept Utilizing Supercritical CO_2 Instead of Water, Geothermal Reservoir Engineering, Stanford, California, 2000.
9. Pruess, K., “Enhanced Geothermal Systems (EGS) using CO_2 as Working Fluid - A Novel Approach for Generating Renewable Energy with Simultaneous Sequestration of Carbon,” Geothermics, n. 35, pp. 351 -367, 2006.
10. Pruess, K., Oldenburg, C. and Moridis, G. “TOUGH2 User's Guide, Version 2.1” Report LBNL-43134, Lawrence Berkeley National Laboratory, Berkeley, CA, 2012.

11. Pruess, K., “On Production Behavior of Enhanced Geothermal Systems with CO_2 as Working Fluid.” Energy Conversion & Management, n. 49, pp. 1446-1454, 2008.
12. Spycher, N. P. K. “A phase-partitioning model for CO_2-brine mixtures at elevated temperatures and pressures. Application to CO_2 enhanced geothermal systems,” Transport in Porous Media, vol. 82, nº 1, pp. 173-196, 2010.
13. Atrens, A. and Gurgenci, H., “CO_2 Thermosiphon for Competitive Geothermal Power Generation,” Energy & Fuels, n. 23, pp. 553-557, 2009.
14. Randolph, J. and Saar, M., “Coupling Geothermal Energy Capture with Carbon Dioxide Sequestration in Naturally Permeable, Porous Geologic Formation: A Comparison with Enhanced Geothermal Systems” GRC Transactions, vol. 34, pp. 1-5, 2010.
15. Randolph, J. and Saar, M., “Coupling Carbon Dioxide Sequestration with Geothermal energy Capture in Naturally Permeable, Porous Geologic Formation: Implications for CO_2 Sequestration,” Energy Procedia, vol. 4, pp. 2206-2213, 2011.
16. Salimi, H. and Wolf, K., “Integration of Heat-Energy Recovery and Carbon Sequestration,” International Journal of Greenhouse Gas Control, vol. 6, pp. 56-68, 2012.
17. Buscheck, T., Chen, M., Sun, Y., Hao, Y. and Elliot, T., “Two-Stage, Integrated Geothermal-CO_2 Storage Reservoirs: An Approach for Sustainable Energy Production, CO_2 Sequestration Security, and Reduced Environmental Risk,” Lawrence Livermore National Laboratory, Livermore, CA, 2012.
18. Zhang, L., Ezekiel, J., Li, D., Pei, J., & Ren, S., “Potential assessment of CO_2 injection for heat mining and geological storage in geothermal reservoirs of China,” Applied Energy 122 (2014), pp. 237-246.
19. Pan, C., Chavez, O., Romero, C., Levy, E., Aguilar-Corona, A. and Rubio-Maya, C., “Heat Mining Assessment for Geothermal Reservoirs in Mexico Using Supercritical CO_2 Injection,” Energy 102 (2016), pp. 148-160.
20. Lehua Pan, Barry Freifeld, etc., “Fully coupled wellbore-reservoir modeling of geothermal heat extraction using CO_2 as the working fluid,” Geothermics 53 (2015), pp. 100-113.

21. Pan, L., Webb, S.W., Oldenburg, C.M., "Analytical solution for two-phase flow in a wellbore using the drift-flux model," Advances in Water Resource 34 (2011a), pp. 1656-1665.
22. Pan L, Oldenburg C M, Pruess K, et al, "Transient CO_2 leakage and injection in wellbore-reservoir systems for geologic carbon sequestration," Greenhouse Gases: Science and Technology 1(4) (2011), pp., 335-350.
23. Pan, L., Wu, Y.-S., Oldenburg, C.M., Pruess, K., T2Well/ECO2N Version 1.0: Multiphase and Non-isothermal Model for Coupled Wellbore-Reservoir Flow of Carbon Dioxide and Variable Salinity Water, LBNL-4291E, 2011c.
24. Pan, L., Oldenburg, C.M., "T2Well-an integrated wellbore-reservoir simulator," Computers and Geosciences 65 (2014), pp. 46-55.
25. Pan, L., N. Spycher, C. Doughty, K. Pruess, "ECO2N V2.0: A TOUGH2 Fluid Property Module for Modeling CO2-H2O-NACL Systems to Elevated Temperatures of up to 300°C." GHG Science and Technology, 7(2) (2017), pp. 313-327.